

UDC 615.012.1:547.79

Anticancer cytotoxicity of indole-thiazolidinone hybrids, *in silico* study of mechanisms of their action

A. P. Kryshchshyn-Dylevych¹, I. Yu. Subtelna¹, N. S. Finiuk²,
L. Radko^{3,4}, A. Pawełczyk⁵, R. S. Stoika², R. B. Lesyk¹

¹ Danylo Halytsky Lviv National Medical University
69, Pekarska Str., Lviv, Ukraine, 79010

² Institute of Cell Biology, NAS of Ukraine
14/16, Drahomanov Str., Lviv, Ukraine, 79005

³ Poznan University of Life Sciences
28, Wojska Polskiego, Poznań, Poland, 60-637

⁴ National Veterinary Research Institute
57, Aleja Partyzantów Puławy, Poland, 24-100

⁵ Poznan University of Medical Sciences
6, Grunwaldzka, Poznań, Poland, 60-780
kryshchshyn.a@gmail.com

Aim. The directed design and synthesis of new hybrid molecules containing [6+5]-heterocycles and thiazolidinone fragment, and their evaluation as potent anticancer agents. **Methods.** Organic synthesis, biological *in vitro* assays, SAR analysis, molecular docking, pharmacophore modelling. **Results.** A series of novel synthetic hybrid thiazolidinone-indole-carboxylates was designed, synthesized, and screened for their toxic activity towards the human hepatocarcinoma (HepG2), human glioblastoma (U251), human breast adenocarcinoma (MCF-7), and human promyelocytic leukemia (HL-60) cell lines. The lines of hepatocarcinoma, glioblastoma and breast adenocarcinoma were weakly sensitive to the studied compounds, the viability of the human promyelocytic leukemia cell line HL-60 was inhibited by 5-fluoro-3-[2-(4-hydroxyanilino)-4-oxo-thiazol-5-ylidene]methyl]-1*H*-indole-2-carboxylate at the micromolar concentration $IC_{50} = 8.36 \mu\text{M}$. The cytotoxic action of this compound tested on a panel of cancer cell lines showed that the cell lines of leukemia, melanoma, and ovarian cancer were the most sensitive to it. **Conclusions.** The *in vitro* screening of biological effects of the synthesized compounds allowed identifying a hit-compound **2c** with high antileukemic action and low toxicity towards pseudonormal murine fibroblasts (Balb/c3T3). In general, 4-thiazolidinone-indolecarboxylate **2c** inhibited by >50 % the viability of 21 tumor cell lines. The *in silico* studies of putative binding mechanisms of the hit-compound **2c** showed its high affinity to the colchicine site of cytoskeletal protein tubulin.

Keywords: 1*H*-indole, thiazolidine, synthesis, anticancer activity, SAR analysis, *in silico* study.

© 2022 A. P. Kryshchshyn-Dylevych *et al.*; Published by the Institute of Molecular Biology and Genetics, NAS of Ukraine on behalf of Biopolymers and Cell. This is an Open Access article distributed under the terms of the Creative Commons Attribution License (<http://creativecommons.org/licenses/by/4.0/>), which permits unrestricted reuse, distribution, and reproduction in any medium, provided the original work is properly cited

Introduction

Development of novel synthetic drug-like molecules requires a selection of pharmacologically attractive, as well as synthetically feasible, starting moieties that would provide potent biologically active compounds. The thiazolidinone and indole heterocycles belong to the scaffolds with proved biological activity, thus, being of interest for the hybrid-pharmacophore application [1, 2]. A combination of indolinone fragment with other 5-membered heterocycles had yielded a series of efficient anticancer drugs, such as Sunitinib that inhibits the activity of tyrosine kinases, including VEGFR, PDGFR and c-KIT [3], Semaxanib — a potent and selective inhibitor of the kinase-insert domain-containing receptor (KDR)/Flk-1 RTK [4], and Orantinib, which acts on multiple members of the split RTK family [5]. Taking into account the efficiency of the above mentioned drugs, the design and synthesis of the small synthetic hybrid molecules based on 3-substituted indole derivatives, and different 5-membered heterocycles as potent anticancer agents present an interesting trend for medicinal chemists [6]. A series of aryl-substituted N-hydroxyindole-2-carboxylates was reported as inhibitors of human lactate dehydrogenase (hLDH5) being a relatively new and untapped anticancer target [7]. A row of 3-indolinone-thiazolidinones and oxazolidinones was described as potent agents for the treatment of renal carcinoma inhibiting the growth of different renal cancer cell lines, as well as exhibiting the inhibition activity towards PDGFR/CDK [8].

5-Fluoro-3-(4-oxo-2-thioxothiazolidin-5-ylidenemethyl)-1*H*-indole-2-carboxylic acid

methyl ester that was previously developed by our scientific group, turned out to be the most potent in a series of alike compounds inhibiting at submicromolar concentrations the viability of more than 50 % of different cancer cell lines (NCI protocol representing a number of neoplastic diseases) [2, 9].

Another direction of search for possible anticancer agents among 4-thiazolidinones is represented by the study of a series of 5-arylidene-2-arylaminothiazol-4(5*H*)-ones on a panel of leukemic cell lines that revealed hit-compounds with IC₅₀ values comparable with those for the control drug Chlorambucil. SAR analysis data showed a high impact of small methoxy and ethoxy groups at position 2 of the benzylidene ring of 5-arylidene-2-arylaminothiazol-4(5*H*)-ones on the antileukemic activity [10]. Thus, here we aimed at the directed structure-based design and synthesis of new hybrid molecules containing [6+5]-heterocycles and thiazolidine ring as potent anticancer agents (Fig. 1).

Materials and Methods

Chemistry

All chemicals were of the analytical grade and commercially available. All reagents and solvents were used without further purification and drying. The starting methyl 5-fluoro-3-formylindole-2-carboxylate and 3-formylindole-2-carboxylic acids were synthesized as described previously [2]. 5-Methoxy-3-(4-oxo-2-thioxothiazolidin-5-ylidenemethyl)-1*H*-indole-2-carboxylic acid **1a** was synthesized in the Knoevenagel reaction according

arom.), 8.06 (d, 1H, $J = 8.62$ Hz, arom.), 8.25 (s, 1H, CH=), 10.53 (s, 1H, NH), 12.63 (bs, 1H, NH). ^{13}C NMR (100 MHz, DMCO- d_6), d : 55.1, 97.0, 115.5, 117.2, 121.4, 125.8, 127.8, 128.8, 129.7, 133.7, 139.7, 161.0, 171.7, 190.1. Calcd for $\text{C}_{14}\text{H}_{10}\text{N}_2\text{O}_4\text{S}_2$: C, 50.29; H, 3.01; N, 8.38; Found: C, 50.45; H, 2.90; N, 8.50.

5,6-Dimethoxy-3-(4-oxo-2-thioxo-thiazolidin-5-ylidenemethyl)-1H-indole-2-carboxylic acid (1c). Yield 75 %, mp 238–240 °C. ^1H NMR (400 MHz, DMSO- d_6), δ : 3.81 (s, 3H, OCH₃), 3.86 (s, 3H, OCH₃), 6.54 (bs, 1H, arom.), 7.09 (bs, 1H, arom.), 8.15 (s, 1H, CH=), 10.48 (s, 1H, NH), 13.63 (bs, 1H, COOH). ^{13}C NMR (100 MHz, DMCO- d_6), d : 55.9, 56.2, 95.4, 102.7, 114.8, 117.4, 124.5, 127.3, 128.5, 131.9, 146.7, 150.1, 162.4, 169.7, 195.5. LCMS (ESI⁺) m/z 365 (M+H)⁺. Calcd for $\text{C}_{15}\text{H}_{12}\text{N}_2\text{O}_5\text{S}_2$: C, 49.44; H, 3.32; N, 7.69; Found: C, 49.90; H, 3.40; N, 7.56.

5-Chloro-3-(4-oxo-2-thioxo-thiazolidin-5-ylidenemethyl)-1H-indole-2-carboxylic acid (1d). Yield 68 %, mp >255 °C. ^1H NMR (400 MHz, DMSO- d_6 +CCl₄), δ : 7.10 (d, 1H, $J = 8.7$ Hz, arom.), 7.21 (s, 1H, arom.), 7.54 (dd, 1H, $J = 2.1, 10.1$ Hz, arom.), 8.28 (s, 1H, =CH), 12.73 (s, 1H, NH), 13.71 (bs, 1H, NH). ^{13}C NMR (100 MHz, DMCO- d_6), d : 108.5, 108.8, 116.5, 116.7, 117.0, 117.7, 126.7, 128.1, 129.6, 135.6, 164.7, 172.3, 198.1. Calcd for $\text{C}_{13}\text{H}_7\text{ClN}_2\text{O}_3\text{S}_2$: C, 46.09; H, 2.08; N, 8.27; Found: C, 46.20; H, 2.15; N, 8.20.

General procedure for synthesis of sodium salt of 5,6-dimethoxy-3-(4-oxo-2-thioxo-thiazolidin-5-ylidenemethyl)-1H-indole-2-carboxylic acid

A mixture of 5,6-dimethoxy-3-(4-oxo-2-thioxo-thiazolidin-5-ylidenemethyl)-1H-indole-2-

carboxylic acid **1c** (0.01 mol) and sodium hydroxide (0.01 mol) in the medium of methanol (20 mL) was stirred at r. t. for 2 h. Formed precipitate was filtered off, washed with ethanol and dried.

Sodium salt of 5,6-dimethoxy-3-(4-oxo-2-thioxo-thiazolidin-5-ylidenemethyl)-1H-indole-2-carboxylic acid (1e). Yield 80 %, mp 226–228 °C. ^1H NMR (400 MHz, DMSO- d_6 +CCl₄), d : 3.82 (s, 3H, OCH₃), 3.86 (s, 3H, OCH₃), 6.82 (s, 1H, arom.), 7.06 (bs, 1H, arom.), 8.17 (s, 1H, CH=), 10.52 (s, 1H, NH). Calcd for $\text{C}_{15}\text{H}_{11}\text{N}_2\text{O}_5\text{S}_2$: C, 49.58; H, 3.05; N, 7.71; Found: C, 49.65; H, 3.00; N, 7.82.

3-[[3-(2-Carboxyethyl)-4-oxo-2-thioxo-thiazolidin-5-ylidene]methyl]-5,6-dimethoxy-1H-indole-2-carboxylic acid (1f). Yield 50 %, mp 228–230 °C. ^1H NMR (400 MHz, DMSO- d_6 +CCl₄), d : 2.62 (t, 2H, $J = 7.6$ Hz, CH₂), 4.22 (t, 2H, $J = 7.6$ Hz, CH₂), 3.79 (bs, 6H, 2*OMe), 6.99 (s, 1H, arom.), 7.20 (s, 1H, arom.), 8.86 (bs, 1H, CH=), 10.73 (bs, 1H, NH), 12.25 (bs, 1H, COOH). Calcd for $\text{C}_{18}\text{H}_{16}\text{N}_2\text{O}_7\text{S}_2$: C, 49.53; H, 3.69; N, 6.42; Found: C, 49.23; H, 3.75; N, 6.50.

General procedure for synthesis of 3-[(2-amino-4-oxo-thiazol-5-ylidene)methyl]-1H-indole-2-carboxylic acid and its derivatives 2a-2b

Method A: A mixture of 2-aminothiazol-4(5H)-one or 2-aryl-aminothiazol-4(5H)-one (0.1 mol), sodium acetate (0.1 mol) and corresponding 3-formyl-1H-indole-2-carboxylic acid or 3-formyl-1H-indole-2-carboxylate (0.11 mol) was refluxed in 100 mL of the acetic acid during 3–5 h. Formed crystalline precipitate was filtered off, washed with acetic acid, water, ethanol, diethyl ether and recryst-

tallized from the mixture DMF/acetic acid (1:2) or acetic acid.

Method B. The mixture of thiourea or arylthiourea (0.1 mol), 3-formyl-1*H*-indole-2-carboxylic acid or 3-formyl-1*H*-indole-2-carboxylate (0.11 mol), chloroacetic acid (0.1 mol) and sodium acetate (0.2 mol) was refluxed in 100 mL of acetic acid for 3–5 h. Formed crystalline precipitate was filtered off, washed with acetic acid, water, ethanol, diethyl ether and recrystallized from mixture DMF/acetic acid (1:2) or the acetic acid.

3-[(2-Amino-4-oxo-thiazol-5-ylidene)methyl]-5-chloro-1*H*-indole-2-carboxylic acid (2a). Yield 74 %, mp >255 °C. ¹H NMR (400 MHz, DMSO-*d*₆+CCl₄), δ: 7.17 (m, 1H, arom.), 7.45-7.49 (m, 2H, arom.), 8.25 (s, 1H, =CH), 8.99 (s, 2H, NH₂), 12.43 (bs, 1H, NH). ¹³C NMR (100 MHz, DMSO-*d*₆), δ: 108.9, 116.7, 117.9, 126.8, 132.0, 132.8, 135.6, 158.2, 161.3, 161.3, 164.9, 177.8, 182.8. Calcd for C₁₃H₈ClN₃O₃S: C, 48.53; H, 2.51; N, 13.06; Found: C, 48.68; H, 2.41; N, 13.14.

3-[[2-(4-Hydroxyanilino)-4-oxo-thiazol-5-ylidene]methyl]-1*H*-indole-2-carboxylic acid (2b). Yield 72 %, mp >255 °C. ¹H NMR (400 MHz, DMSO-*d*₆+CCl₄), δ: 6.70 (d, 1H, *J* = 7.8 Hz, arom.), 6.80 (d, 1H, *J* = 8.0 Hz, arom.), 6.88 (d, 1H, *J* = 7.8 Hz, arom.), 7.12 (dt, 1H, *J* = 7.2, 26.2 Hz, arom.), 7.30 (dt, 1H, *J* = 7.7, 26.9 Hz, arom.), 7.47-7.55 (m, 2H, arom.), 7.85 (d, 1H, *J* = 7.8 Hz, arom.), 8.25, 8.38 (2*s, 1H, =CH), 9.53 (2bs, 1H, OH), 11.18 (bs, 1H, NH), 12.37, 12.4 (2*s, 1H, NH), 13.02 (bs, 1H, COOH). ¹³C NMR (100 MHz, DMSO-*d*₆), δ: 113.8, 115.2, 115.9, 116.3, 121.3, 122.6, 123.9, 124.5, 125.6, 127.7, 128.0, 129.0, 130.8, 136.8, 155.2, 155.6, 162.8, 169.9, 180.6. Calcd for C₁₉H₁₃N₃O₄S: C, 60.15; H,

3.45; N, 11.08; Found: C, 60.30; H, 3.60; N, 10.96.

Pharmacology

Cell line culturing. *In vitro* screening of anticancer activity of synthesized compounds was carried out at the National Cancer Institute (USA) within the Developmental Therapeutic Program (www.dtp.nci.nih.gov). Anticancer assays were performed according to the US NCI protocol described elsewhere [12–14]. Part of the study (cytotoxicity: HepG2 and Balb/c 3T3 cells) was carried out at the National Veterinary Institute — National Research Institute in Pulawy, Poland.

Human hepatoma HepG2 cell line was purchased from the American Type Culture Collection (ATCC HB-8065). The cells were cultured in the Minimum Essential Medium Eagle (MEME) (ATCC, USA). The murine fibroblasts cell line (Balb/c 3T3 clone A31) (a gift of the Department of Swine Diseases of the National Veterinary Research Institute in Pulawy, Poland) was cultured in the Dulbecco's Modified Eagle's Medium (DMEM) (ATCC, USA). Human breast adenocarcinoma MCF-7 cells, human glioblastoma U251 cells, and human acute promyelocytic leukemia HL-60 cells were obtained from the Cell Collection of R.E. Kavetsky Institute of Experimental Pathology, Oncology and Radiobiology (Kyiv, Ukraine). The cells were cultured in the DMEM (BioWest, France) or the RPMI-1640 media (BioWest, France) supplemented with 10 % BCS (Balb/c 3T3), 10 % FBS (other cell lines), 1 % L-glutamine, and 1 % antibiotic solution. The cells were maintained in 75 cm² plastic flasks (NUNC, Denmark) in a humidified incubator at 37 °C,

in an atmosphere of 5 % CO₂. The medium was made fresh every two or three days, and the cells were treated with 0.25 % trypsin/0.02 % EDTA after reaching 70–80 % confluence. Single cell suspensions were prepared and adjusted to a density of 2×10^5 cell/mL (HepG2) and 1×10^5 cell/mL for 24 h, 48 h exposition or 5×10^4 cell/mL for 72 h exposition (adherent cells), or 10×10^5 cell/mL for 72 h exposition (HL-60 cells). The cell suspension was transferred to 96-well plastic plates (100 μ L/well) and incubated for 24 h before exposure to the studied compounds. The stock solution of study compound was prepared in the DMSO and diluted with culture medium to obtain a concentration range from 10^{-2} – 10^2 μ M (HepG2 and Balb/c 3T3). Part of cells was also exposed to the reference anticancer drugs — Cisplatin (Sigma-Aldrich, USA) or Doxorubicin (Actavis, Romania). The final concentration of DMSO was ≤ 0.1 % in the medium and had no influence on cell growth. The medium used for test solutions and in control preparation did not contain blood serum and antibiotics. In the negative control, cultured cells were grown in the absence of studied compound. Each concentration was tested in six replicates with three independent experiments. Cytotoxicity was assessed after 24, 48 and 72 h of cell exposure to the compounds. During the incubation time, the medium was not changed. Cytotoxicity was assessed using: MTT, NRU, TPC and LDH assays.

The MTT assay of cell viability in vitro. The metabolic activity of the living cells was assessed by measuring the activity of the mitochondrial dehydrogenases [15, 16]. After incubation of cells with the studied compound,

10 μ L of the MTT solution (5 mg/mL in PBS) were added to each well of 96-well plastic plates and incubated. After 3 h incubation, the MTT solution was removed and the formed intracellular formazan crystals were dissolved in 100 μ L DMSO. The plate was shaken for 15 min at room temperature and transferred to a microplate reader (Synergy HTX multi-mode reader (BioTek® Instruments Inc., USA)) to measure the absorbance at 570 nm, using blank as a reference. Cytotoxicity value was expressed as a percentage of the negative control (0.1 % DMSO) [17].

Neutral red uptake (NRU) assay. The method is based on staining living cells with neutral red that readily diffuses through the plasma membrane and accumulates in the lysosomes [18]. After the incubation, the medium containing the drug was removed and the cells were washed with the PBS solution. Then, 100 μ L/well of NR solution (50 μ g/mL) were added for 3 h. After the incubation, the cells were washed with the PBS. The dye from the viable cells was released by extraction with a mixture of acetic acid, ethanol and water (1:50:49, v:v:v). After 10 min shaking, the absorbance of the dissolved NR was measured using Synergy HTX multi-mode reader (BioTek® Instruments Inc., USA) at 540 nm with blank as a reference. Cytotoxicity level was expressed as a percentage of the negative control (0.1 % DMSO) [17].

Total cellular protein (TCP) assay. The assay is based on staining total cellular protein (corresponding to cell proliferation) [19]. After incubation, the medium containing drug was removed and 100 μ L of the Coomassie brilliant blue R-250 dye were added to each well. The plate was shaken for 10 min. Then, the staining

solution was removed and the cells were rinsed twice with 100 μ L of washing solution (glacial acetic acid/ethanol/water, 5:10:85, v:v). After that, 100 μ L of the desorbing solution (1 M potassium acetate) were added, and plates were shaken for 10 min. The absorbance was measured at 595 nm in a microplate reader (Synergy HTX multi-mode reader (BioTek® Instruments Inc., USA)) using blank as a reference. Cytotoxicity level was expressed as a percentage of the negative control (0.1 % DMSO) [17].

Lactate dehydrogenase (LDH) leakage assay. The integrity of plasma membrane was assessed through the test of lactate dehydrogenase (LDH) release [20], which was monitored using the commercially available Cytotoxicity Detection Kit (LDH) (Roche Diagnostics, Poland). The medium (100 μ L/well) without cells was transferred into the corresponding wells of an optically clear 96-well flat bottom microplate and 100 μ L reaction mixture was added to each well. Then, the plates were incubated in darkness for 30 min at room temperature. After that, 50 μ L/well of 1 M HCl was added to stop the reaction. The absorbance was measured at 492 nm on a microplate reader (Synergy HTX multi-mode reader (BioTek® Instruments Inc., USA)) using blank as a reference [17].

Selectivity index. To determine the cytotoxic selectivity of the tested compound, the selectivity index (SI) was calculated according to the following equation: $SI = GI_{50} \text{ for non-cancer cells} / GI_{50} \text{ for cancer cells}$ where a $SI \geq 3$ was considered to belong to a selective compound [21]. The compounds displaying the SI above 10 are considered to be highly selective [22]. A beneficial $SI > 3.0$ indicates

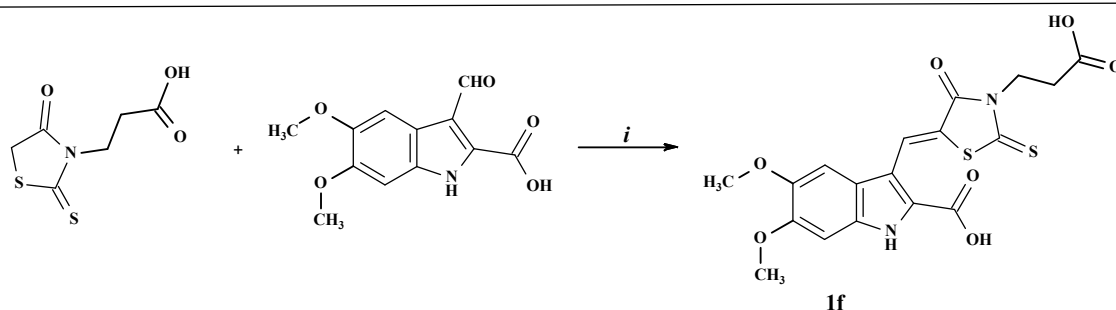
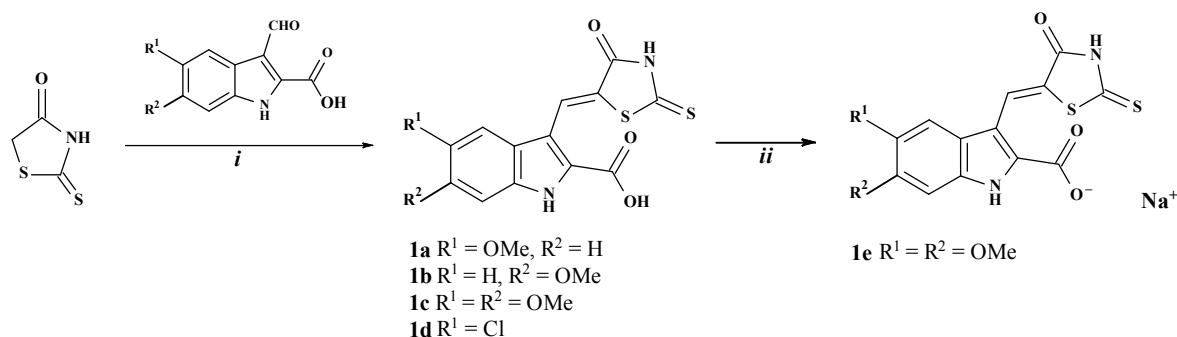
a drug with the efficacy against tumor cells greater than toxicity against normal cells. For calculating the SI values, the $GI_{50} > 100 \mu\text{M}$ was taken as being 100 μM . The cytotoxicity level was expressed as the mean arithmetical values from three independent experiments. The percentage of the viability inhibition was calculated in comparison with the untreated controls. The GI_{20} , GI_{50} , GI_{80} values (growth inhibition concentrations), the compounds concentrations that reduce the cell growth by 20 %, 50 % and 80 %, were calculated by GraphPad Prism 5 software (San Diego, CA, USA) using nonlinear regression.

In silico studies. The molecular docking simulations were performed to assess the affinity of the synthesized compounds to Human VEGF receptor, Tubulin (PDB codes: 6XER, 6WVR, 5J2T), RNase L (PDB codes: 6M11, 6M13), KIT kinase (PDB code: 3G0E) and Abl kinase (PDB code: 3K5V). 2D structures of the synthesized ligand molecules were drawn by Biovia Draw v.21.1 and converted to energy-minimized 3D structures by Hyperchem 7.5 [23]. The X-ray crystallographic structures of the above mentioned Human VEGF receptor (PDB code: 5EWR) [24], Tubulin (PDB codes: 6XER, 6WVR, 5J2T) [25–27], RNase L (PDB codes: 6M11, 6M13) [28], KIT kinase (PDB code: 3G0E) [29] and Abl kinase (PDB code: 3K5V) [30] were retrieved from the protein data bank. Molecular docking simulations using the ligand molecules were conducted using the Autodock 4.2.6 docking suite by employing the Lamarckian genetic algorithm [31]. The preparations of proteins and further processing of ligand data were done in the AutoDock Tools suite. Before docking, the protein crystal structures were

cleaned by removing the water molecules and other inclusions. Polar H-atoms were added to these target proteins for correct ionization and tautomeric states, and non-polar H-atoms were merged. Docked ligands were set as flexible and the Gasteiger charges were added to them. The grid maps representing the center of active site pockets for the ligand were calculated using the Autogrid Tools. The grid dimensions for all tested macromolecules were 60*60*60 points with a spacing of 0.375 Å between the grid points. 50 Docking experiments were performed and the best-docked conformation was selected based on the free binding energy (kcal/mol) and Inhibition Constant (K_i) for further analysis. Data obtained from the redocking procedures were used for quantitative

estimating of ligands affinity to our targets and compared to established agonists. Finally, the conformations with the most favorable free binding energy were selected for analyzing the interactions between the target macromolecules and ligands by Chimera 1.16 [32] and AutoDock Tools suite.

Pharmacophore modelling was performed using the LigandScout 4.4.7 [33]. For this purpose, the same complexes AAL993 — Human Vascular Endothelial Growth Factor Receptor (5EW3), Sunitinib — RNase L (6M11), Toceranib — RNase L, (6M13), Colchicine — Tubulin (Colchicine site, 6XER), Paclitaxel — Tubulin (Taxol site, 6WVR), Vinblastin — Tubulin (Vinblastin site, 5J2T), as for molecular docking studies were selected.



Scheme 1. Synthesis of 3-(4-oxo-2-thioxothiazolidin-5-ylidene)methyl-1*H*-indole-carboxylic acids **1a-1f**.

Reagents and conditions: *i*) 3-formyl-1*H*-indol-2-carboxylic acid (1.0 equiv) and 4-thioxo-2-thiazolidinone (1.0 equiv), sodium acetate (1.0 equiv), AcOH, reflux 2.5 h; *ii*) **1c** (1.0 equiv), NaOH (1.0 equiv), MeOH, rt, 2h

The binding sites from each protein were sources for Pharmacophore models formation, that were later compared to 3D structure model of studied compound **2c**. The pharmacophore model similarity is expressed by numeric parameter Pharmacophore-Fit Score.

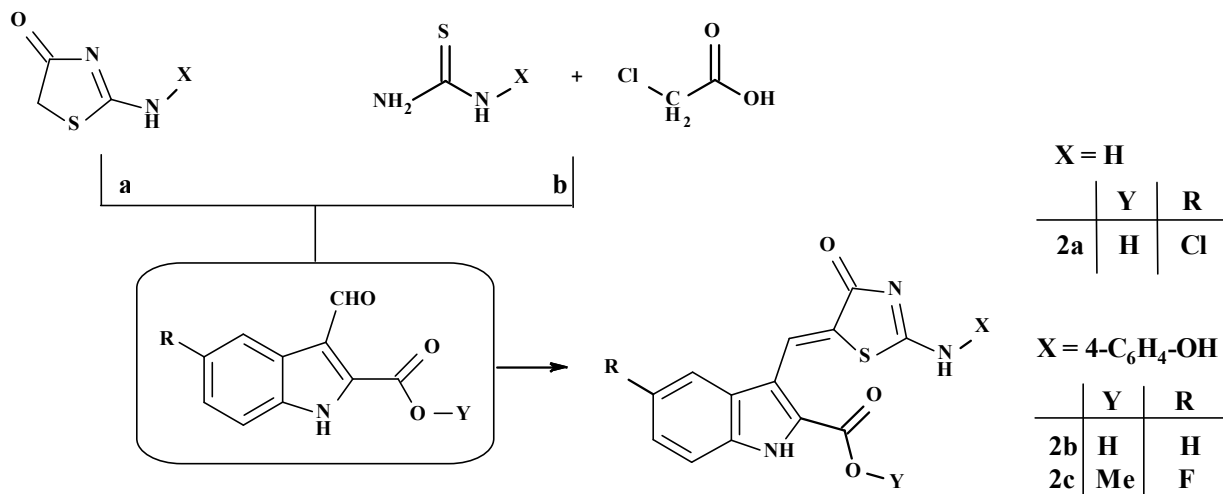
Results and Discussion

Chemistry

Design of target compounds was based on the combination of methoxy and halogen substituted 1*H*-indole-2-carboxylic acids with 2-thioxothiazolidin-4-one (**1a-1f**). Compounds **1a-1f** were synthesized in the Knoevenagel reaction in the acetic acid medium with adding equimolar quantities of sodium acetate (Scheme 1). Fragment of rhodanine-3-carboxylic acid had been chosen for hybrid molecules

design as 5-ene-rhodanine-carboxylic acids showed high antibacterial, antiparasitic, as well as anticancer activity [34, 35]. So, the Knoevenagel reaction of 5,6-dimethoxy-1*H*-indole-2-carboxylic acid with rhodanine-3-carboxylic acid yielded hybrid molecule **1e** (Scheme 1).

3-[(2-Amino-4-oxo-thiazol-5-ylidene)methyl]-1*H*-indole-2-carboxylic acids **2a-2c** were synthesized in one-pot three-component reaction of substituted thioureas (S,N-binucleophiles), chloroacetic acid as electrophile and appropriate oxo compound in the acetic acid medium. Given method includes the reaction of [2+3]-cyclocondensation followed by Knoevenagel condensation (method *a*) that allows significant reduction for the time of the target compounds synthesis and amounts of reagents used on the contrary to two independent reactions of 2-heterylimino-4-thiazolidi-



Scheme 2. Synthesis of 3-[(2-amino-4-oxo-thiazol-5-ylidene)methyl]-1*H*-indole-2-carboxylic acid and its derivatives **2a-2c**.

Reagents and conditions: **Method a**: 2-aminothiazol-4(5*H*)-one or 2-aryl-aminothiazol-4(5*H*)-one (1.0 equiv), 3-formyl-1*H*-indole-2-carboxylic acid or 3-formyl-1*H*-indole-2-carboxylate (1,1 equiv), AcOH, reflux 3-5 h; **Method b**: thiourea or arylthiourea (1.0 equiv), 3-formyl-1*H*-indole-2-carboxylic acid or 3-formyl-1*H*-indole-2-carboxylate (1,1 equiv), chloroacetic acid (1.0 equiv), sodium acetate (2.0 equiv) acetic acid, reflux 3-5 h.

nones and their 5-ene derivatives synthesis (method **b**) [36–38] (Scheme 2).

The purity and structure of synthesized compounds were confirmed by the analytical and spectral data. ^1H and C^{13}NMR spectra of compounds **2a–2c** showed characteristic multiplication of signals because of the existence of two different tautomeric forms. Synthesized 2-substituted 4-thiazolidinones **2a–2c** can exist as a mixture of two tautomers that differ by the position of $\text{C}=\text{N}$ double bond (2-amino- and 2-imino tautomers); tautomers with exocyclic $\text{C}=\text{N}$ double bond exist as a

mixture of *Z*- and *E*-stereoisomers. The prototropic tautomerism and stereoisomerism for such compounds were previously studied both in solutions and in the solid state [36, 39]. Structural features of synthesized compounds and prevalent existence of 2-arylaminothiazol(5H) 4-ones in crystals in amino form were confirmed by X-ray crystallographic analysis of similar compounds [36, 40–42]. The presence of the signal of $\text{CH}=\text{N}$ group (singlet, for 5-ylidene compounds) at $\sim 8.15\text{--}8.86$ ppm confirms the formation of compounds with *cis*-orientation of ylidene

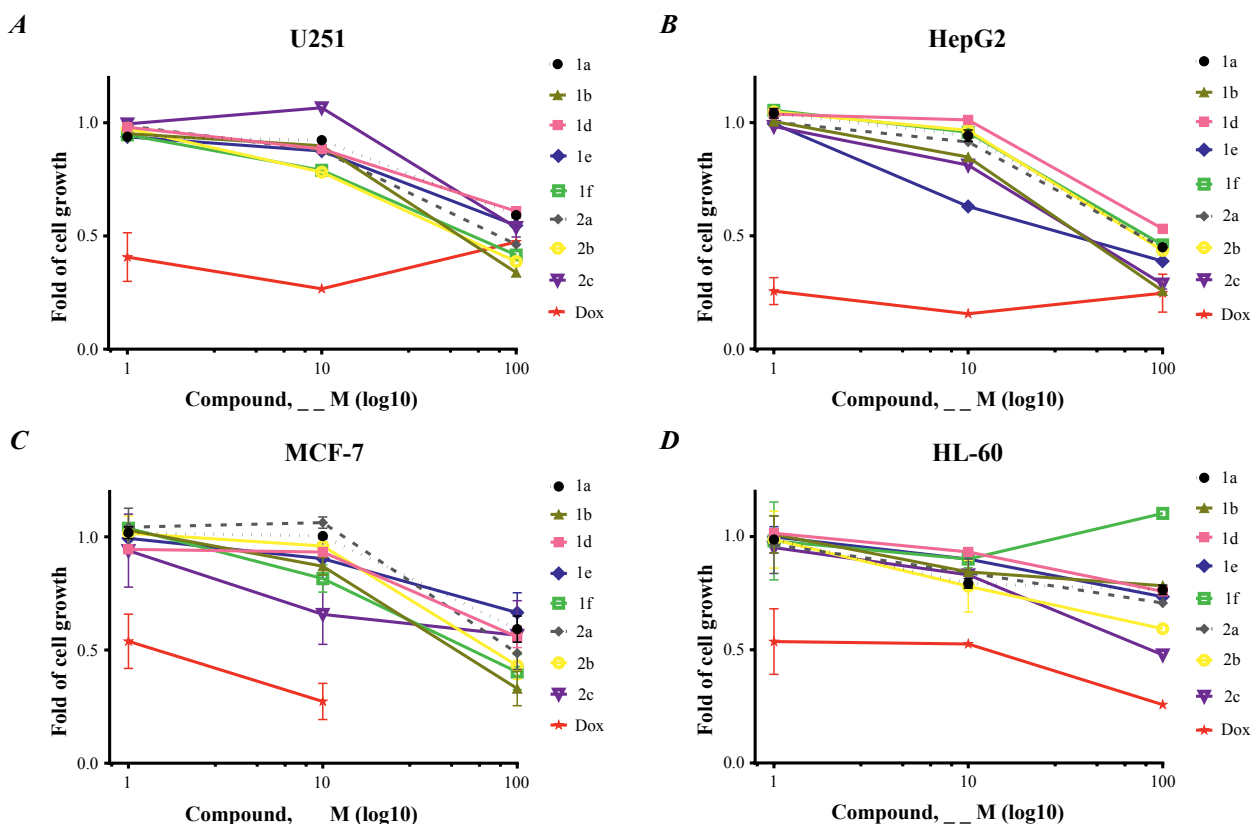


Fig. 2. Concentration-dependent cytotoxic effect of the studied derivatives and Doxorubicin (Dox) towards human hepatocarcinoma (HepG2), human glioblastoma (U251), human breast adenocarcinoma (MCF-7), and human promyelocytic leukemia (HL-60) cell lines for 72 h. Results of the MTT assay are presented as $\text{M} \pm \text{SD}$ ($n = 6$).

residue (*Z*-configuration), similar to other 5-ene-4-azolidinones [36, 41].

Anticancer activity

The synthesized novel hybrid thiazolidinone-indole-carboxylates were screened for the anticancer activity towards a panel of cancer cell lines including human hepatocarcinoma (HepG2), human glioblastoma (U251), human breast adenocarcinoma (MCF-7) and human promyelocytic leukemia (HL-60) cell lines (Fig.2, Table 1).

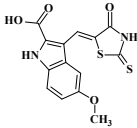
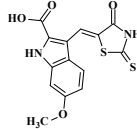
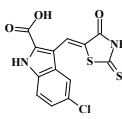
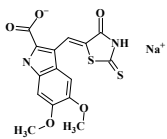
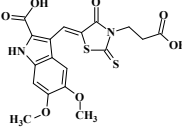
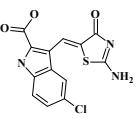
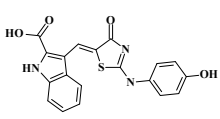
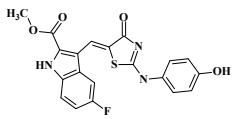
In general, the lines of human hepatocarcinoma, glioblastoma and breast adenocarcinoma were not highly sensitive to studied thiazolidinone-indole-carboxylic acid and 2-amino-4-oxo-thiazol-indole-carboxylic acid derivatives. The IC_{50} concentrations on the glioblastoma line U251 were 50.4 μ M and 50.5 μ M for **1b** and **2b**, respectively. At a close concentration of 47.8 μ M, the compound **1b** inhibited the viability of breast adenocarcinoma MCF-7 cells (Fig. 2, Table 1). Human hepatocarcinoma HepG2 line with the lowest IC_{50} values of 38.6 μ M, 32.6 μ M, and 38.1 μ M, for **1b**, **1e** and **2c**, respectively, were found to be the most sensitive cancer cell line to the action of studied class of compounds. Introduction of chlorine atom in the indole ring did not contribute to the inhibition activity of the compounds **1d** and **2a** on cancer cell viability. Molecules with methoxy substituents in the indole fragment showed lower IC_{50} values, especially against human hepatocarcinoma HepG2 line. Increasing solubility in a form of 5,6-dimethoxy-3-(4-oxo-2-thioxothiazolidin-5-ylidenemethyl)-1*H*-indole-2-carboxylic acid sodium salt **1e** also had not significant impact on the anticancer activity, since the IC_{50} on HepG2 cells

were at the same range as for the compounds **1b** and **2c**. Micromolar range of IC_{50} (8.4 μ M) of 5-fluoro-3-[2-(4-hydroxyanilino)-4-oxo-thiazol-5-ylidene]methyl]-1*H*-indole-2-carboxylate (compound **2c**) was comparable with that (1.7 μ M) for the reference drug Doxorubicin at their action on human promyelocytic leukemia cells of HL-60 line.

The cytotoxic action of the hit-compound and the compounds **1b**, **1d**, **2a** and **2b** was investigated at 10 μ M concentration according to the NCI protocol (Table 2) [12–14]. The results for each test agent were reported as the percent growth (GP) of the treated cells compared to the untreated control cells. Among these four compounds, only **1b** inhibited viability of melanoma cell line MDA-MB-435 by more than 70 %, whereas other three compounds were only slightly active towards one cell line of renal cancer UO-31. The most sensitive to the action of **2c** were leukemia cell lines whose viability was inhibited by more than 50 %, melanoma line MDA-MB-435 (GP = 0.95 %), ovarian cancer cell line OVCAR-3 (GP = 19.82 %) and breast cancer line MCF7 (GP = 22.03 %). In general, 4-thiazolidinone-indolecarboxylate **2c** inhibited the viability of 21 tumor cell lines by more than 50 %.

For the identified hit-compound **2c**, the cytotoxicity towards human hepatocellular carcinoma cells HepG2 and pseudonormal murine fibroblasts Balb/c 3T3 was additionally studied. Different *in vitro* methods were used for the cytotoxic action study of **2c** at 24, 48 and 72 h exposition of the targeted cells: 1) MTT assay for the activity of mitochondrial dehydrogenases; 2) NRU assay for lysosomal activity; 3) TPC assay for evaluation of

Table 1. Results of anticancer activity study towards four cancer cell lines

Comp.	Structure	IC ₅₀ , μM			
		U251	HepG2	MCF-7	HL-60
1a		>100	78.1 \pm 0.5	>100	>10
1b		50.4 \pm 0.3	38.6 \pm 0.5	47.8 \pm 1.1	>10
1d		>100	>100	>100	>10
1e		>100	32.6 \pm 0.6	>100	>10
1f		57.3 \pm 0.3	82.5 \pm 0.5	56.9 \pm 0.2	>10
2a		80.9 \pm 0.9	74.3 \pm 0.1	92.4 \pm 0.6	>10
2b		50.5 \pm 0.4	76.0 \pm 0.5	72.2 \pm 0.9	>10
2c		>100	38.1 \pm 0.2	>100	8.4 \pm 0.2
Doxorubicin		0.8	0.8 \pm 0.1	0.6 \pm 0.1	1.7 \pm 0.1

HepG2 — human hepatocarcinoma, U251 — human glioblastoma, MCF-7 — human breast adenocarcinoma, and HL-60 — human promyelocytic leukemia

total protein content; 4) LDH assay for estimation of integrity of cellular membrane. The antiproliferative activity of 5-fluoro-3-[[2-(4-hydroxyphenyl)imino-4-oxo-thiazolidine-5-ylidene]methyl]-1*H*-indole-2-carboxylate **2c** was detected after 24 h of incubation at a concentration of 0.0001 μM , whereas the toxic effect on normal cells was observed at a higher concentration of 0.1 μM .

Noteworthy, at 48 and 72 h of exposure, the observed active concentrations for cancer cells

were as low as 0.00001 μM . The calculated cytotoxicity concentrations (GI_{20} , GI_{50} and GI_{80}) towards HepG2 and normal cells are presented in Table 3. The lowest sub-micromolar concentration values (GI_{20}) were observed in LDH and NRU tests at all time points. The initial stage of the cytotoxic effect of compound **2c** was the disintegration of the cell membrane of cancer cells, which leads to the inhibition of their lysosomal activity. It is important to note that the tested compound **2c**

Table 2. Anticancer screening data (one dose assay, 10 μM)

Comp.	Mean growth %	Range of growth %	The most sensitive cell lines	GP% of the most sensitive cell lines	Positive cytostatic effect*
1b	83.01	28.30 to 109.80	K-562/ <i>L</i> SR/ <i>L</i> SNB-75/ <i>CNSC</i> MDA-MB-435/ <i>M</i>	53.66 56.49 42.97 28.30	2/57
1d	99.73	75.73 to 115.40	UO-31/ <i>RC</i>	75.73	0
2a	101.67	75.18 to 117.05	UO-31/ <i>RC</i>	75.18	0
2b	99.72	73.62 to 116.79	UO-31/ <i>RC</i>	73.62	0
2c	61.85	0.95 to 106.28	CCRF-CEM/ <i>L</i> K-562/ <i>L</i> SR/ <i>L</i> HOP-92/ <i>NscLC</i> SNB-19/ <i>CNSC</i> U251/ <i>CNSC</i> MDA-MB-435/ <i>M</i> UACC-62/ <i>M</i> OVCAR-3/ <i>OC</i> A498/ <i>RC</i> RXF 393/ <i>RC</i> MCF7/ <i>BC</i> BT-549/ <i>BC</i>	28.17 23.19 24.19 42.69 45.70 46.45 0.95 34.30 19.82 42.37 43.64 22.03 35.01	21/60

* Ratio between number of cell lines with percent growth from 0 to 50 and total number of cell lines.

L — Leukemia; *NscLC*— Non-Small Cell Lung Cancer; *BC* — Breast cancer; *CC* — Colon Cancer; *OC* — Ovarian Cancer; *RC* — Renal cancer; *M* — Melanoma; *CNSC* — CNS Cancer

Table 3. Calculated values of cytotoxic concentrations (GI₂₀; GI₅₀; GI₈₀)^a for the compound **2c in the tests on HepG2 and pedsnormal fibroblasts of Balb/c 3T3 line**

Cell line	Method	Time (h)	GI ₂₀ , μM	GI ₅₀ , μM	GI ₈₀ , μM
Balb/c 3T3	MTT	24	3.3±0.3	9.7±0.2	>100
		48	2.8±0.4	7.5±0.6	>100
		72	2.5±0.8	7.4±0.8	>100
	NRU	24	6.3±1.1	>100	>100
		48	5.4±1.2	>100	>100
		72	2.5±0.9	27.8±3.8	>100
	TPC	24	72.2±6.0	>100	>100
		48	0.07±0.02	>100	>100
		72	0.06±0.01	44.4±3.4	>100
	LDH	24	>100	>100	>100
		48	21.6±2.6	83.6±3.2	>100
		72	0.4±0.1	9.6±0.5	>100
HepG2	MTT	24	2.1±0.9	8.0±0.4	>100
		48	1.6±0.5	6.7±0.3	>100
		72	0.4±0.3	5.5±0.3	16.5±2.4
	NRU	24	0.8±0.05	34.4±2.6	87.3±2.3
		48	0.07±0.03	20.9±1.0	76.1±1.4
		72	0.0007±0.0001	8.4±1.1	64.4±2.2
	TPC	24	15.4±2.5	>100	>100
		48	0.05±0.001	23.4±2.5	>100
		72	0.01±0.0003	9.6±0.2	>100
	LDH	24	0.07±0.01	0.9±0.05	12.5±3.1
		48	0.0005±0.00003	0.07±0.01	6.8±0.6
		72	0.0002±0.00004	0.0009±0.0001	6.3±1.4

* GI₂₀, GI₅₀ and GI₈₀ (μM) represent the concentrations of the studied compound that are required for 20, 50 and 80 % inhibition of the cell viability using the MTT, NRU, TPC and LDH assays. Data are presented as the mean \pm SEM from the dose response curves of at least three independent experiments.

showed low toxicity against the normal cell line of murine embryo fibroblasts (Balb/c3T3), and the mechanism of cytotoxicity towards them can be established through mitochondrial dysfunction. The compound **2c** was characterized by high SI values (> 3.0) not only in the LDH test, but also in the NRU at all time points, as well as in the TPC test after 48 and

72 h of exposure. SI values for the LDH assay were higher compared to SI values for the reference drug cisplatin by 11 %, 16 %, and 9 % at 24, 48, and 72 h, respectively (Fig. 3).

To study the putative binding mechanisms of identified hit-compound **2c**, a panel of bio-targets was selected for *in silico* studies. The results of a number of biological assays per-

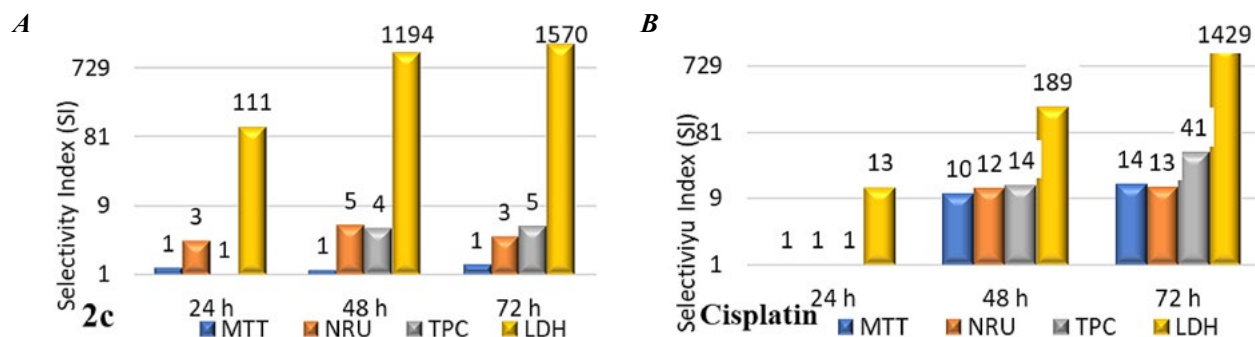


Fig. 3. Calculated Selectivity Indices (SI) for the compound **2c** compared to the SI for Cisplatin towards HepG2 cells.

formed earlier for the compound **2c** showed that it did not influence the metabolic activity of healthy fibroblasts and could not induce apoptosis in normal and cancer cells [11], however, it had the prooxidative effect on the cancer cell lines (BJ, A549, and SH-SY5Y) [43]. So, the bio-targets involved in the molecular mechanisms of the apoptotic signaling pathway were not included in the *in silico* studies.

On the other hand, the hit-compounds established as a result of the antileukemic activity study of a series of 5-arylidene-2-(4-hydroxyphenyl)aminothiazole-4(5*H*)-ones were shown to induce mitotic arrest by the interacting with tubulin and inhibiting its polymerization via binding to the colchicine binding site [10, 44]. Therefore, tubulin was chosen as one of the bio-targets for the molecular docking study. Based on structure likeness of Sunitinib and Toceranib to the compound **2c**, the pseudokinase RNase L — a functional ribonuclease inhibited by above drugs [28], has been also selected for the computational studies. One more complex of Abl kinase with Imatinib — a protein kinase inhibitor used to treat a number of leukemias [30], was chosen as a possible bio-target for *in silico* study of **2c** binding mode.

Docking simulation showed high affinity of the hit-compound **2c** to colchicine site in tubulin (−10.22 kcal/mol) confirming experimental results for a group of 5-arylidene-2-(4-hydroxyphenyl)aminothiazole-4(5*H*)-ones [44] and indicating the crucial role of the 2-(4-hydroxyphenyl)aminothiazol fragment for binding mode of alike molecules in this site. Moreover, the calculated binding energy with tubulin (colchicine site) for the compound **2c** was higher than for colchicine (−9.12 kcal/mol). We have found four H-bonds between **2c** and intrasubunit interface in tubulin comprised of α and β subunits, namely THR179 and VAL181 in α subunit and VAL236 and ASP249 in β subunit (Fig. 4, Table 4). Also, 5-fluoro-3-[2-(4-hydroxyanilino)-4-oxo-thiazol-5-ylidene]methyl]-1*H*-indole-2-carboxylate **2c** showed high affinity to RNase L with even lower binding energy (−9.58 kcal/mol) compared with calculated binding energy for Sunitinib (−9.17 kcal/mol). Besides, we found six H-bonds formed with GLN486, ASP500 and CYS435 of RNase L, respectively (Table 4).

For the in-depth *in silico* study of **2c**, the Pharmacophore modelling was performed us-

Table 4. Results of molecular docking calculated for the compound **2c**

Protein/Ligand	PDB code	Binding energy (kcal/mol)		Inhib. const. (Ki), μM	Number of H bonds	Amino acids involved in interactions (length, Å)
		ligand	2c			
VEGFR*/AAL993	5ew3	-13.18	-9.10	0.213	3	ALA881-NH (2.016 Å); ARG1027-COO (1.74 Å); LYS868-OH (2.022 Å)
Tubulin/Colchicine	6xer	-9.12	-10.22	0.032	4	THR179(a)-NH ind. (1.957 Å); VAL236(b)-OH (1.901 Å); ASP249(b)-NH (2.182 Å) VAL181(a)-COO (2.283 Å)
Tubulin/Paclitaxel	6wvr	-6.56	-6.34	22.36	2	ARG278(b)-COO (1.875 Å); ARG278(b)-CO thiaz. (2.183 Å)
Tubulin/Vinblastin	5j2t	-12.66	-7.78	1.97	4	VAL177(b)-NH (2.086 Å); ASN329(c)-CO het (2.342 Å); ASN329(c)-COMe (1.963 Å); TYR224(b)-OH (2.030 Å)
RNase L/Sunitinib	6m11	-9.17	-9.58	0.094	6	GLN486(b)-OH (2.041 Å); ASP500(b)-NH (2.005 Å); ASP500(b)-NH thiaz. (2.397 Å); ASP500(b)-NH thiaz. (1.890 Å); CYS435(b)-COO (1.886 Å); CYS435(b)-NH ind. (1.963 Å)
RNase L/Toceranib	6m13	-10.20	-8.41	0.680	4	GLN486(b)-OH (2.073 Å); ASP500(b)-NH thiaz. (1.837 Å); CYS435(b)-COMe (2.121 Å); CYS435(b)-NH ind. (2.397 Å)
KIT kinase/Sunitinib	3g0e	-8.18	-6.20	28.77	0	-
Abl kinase/Imatinib	3k5v	-11.83	-9.25	0.166	1	GLU305-NH (1.959 Å)

ing the same bio-targets as for the molecular docking. During screening, the minimum number of features at which the model and the studied molecules should match had been set. The results of pharmacophore modeling of compound **2c** are presented in Table 5. The highest pharmacophore-fit score for **2c**, compared with such one for the initial ligand, was calculated for pharmacophore derived from the colchicine binding site of tubulin that correlates with our previous studies [44], as well as

with the levels of binding energy obtained in a molecular docking study.

In silico simulations reveal that the hit-compound **2c** possesses a potential affinity to the colchicine site of tubulin, as well as the bio-targets for the Sunitinib, such as RNase L and KIT kinase.

Conclusion

A series of hybrid molecules containing indole cycle and 2-thioxo-thiazolidinone-4 or 2-ami-

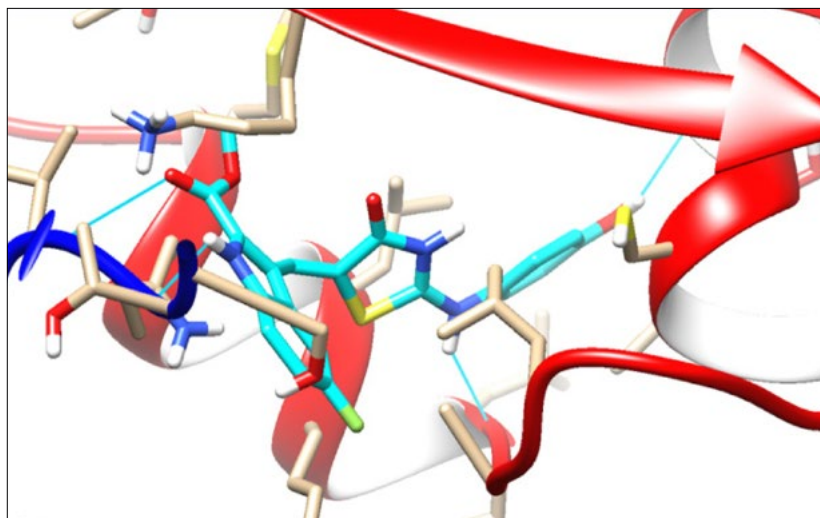


Fig. 4. Interaction of the compound **2c** with the colchicine binding site of tubulin (PDB code: 6XER); subunit α — blue, subunit β — red; 4 H bonds — cyan.

no(imino)-thiazolidinone-4 fragments was designed and synthesized. *In vitro* screening of the biological effects of synthesized com-

pounds allowed identifying a hit-compound 5-fluoro-3-[2-(4-hydroxyanilino)-4-oxo-thiazol-5-ylidene]methyl]-1*H*-indole-2-carboxy-

Table 5. Calculated Pharmacophore-Fit scores for the hit-compound **2c**

Protein	PDB code	Pharmacophore-Fit Score		(number of omitted features)
		Ligand	2c	
Human Vascular Endothelial Growth Factor Receptor	5ew3	<i>AAL993</i>		
		61.66	36.80	4
Tubulin (Colchicine site)	6xer	<i>Colchicine</i>		
		36.78	38.34	1
Tubulin (Taxol site)	6wvr	<i>Paclitaxel</i>		
		87.47	-	
Tubulin (Vinblastin site)	5j2t	<i>Vinblastin</i>		
		106.95	-	
RNase L	6m11	<i>Sunitinib</i>		
		86.05	55.73	3
RNase L	6m13	<i>Toceranib</i>		
		76.28	46.88	3
KIT kinase	3g0e	<i>Sunitinib</i>		
		67.02	47.22	2
Abl kinase	3k5v	<i>Imatinib</i>		
		107.43	-	

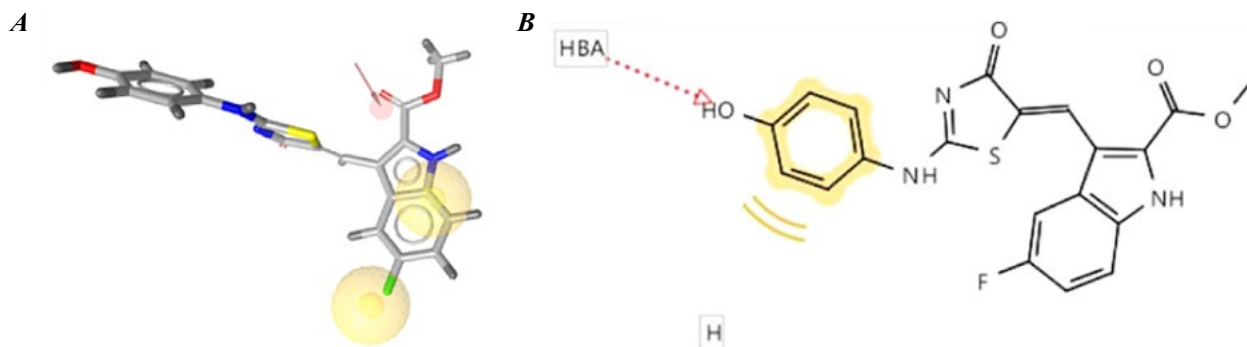


Fig. 5. Overlaying of the compound **2c** with pharmacophore model (yellow spheres and red arrow) derived from colchicine (tubulin PDB code: 6XER, colchicine site).

late (**2c**) that was highly active against leukemia cell lines and melanoma line MDA-MB-435 and was characterized by low toxicity towards pseudonormal murine fibroblasts (Balb/c3T3). The results of molecular docking and pharmacophore modelling studies suggest the affinity of the hit-compound **2c** to the colchicine site of tubulin, however, further experimental studies are needed to establish the molecular mechanism of its action.

Acknowledgment

Molecular graphics and analyses are performed with UCSF Chimera, developed by the Resource for Biocomputing, Visualization, and Informatics at the University of California, San Francisco, with support from NIH P41-GM103311.

REFERENCES

1. Kryshchyshyn A, Kaminsky D, Karpenko O, Gzella A, Grellie, P, Lesyk R. Thiazolidinone/thiazole based hybrids—New class of antitrypanosomal agents. *Eur J Med Chem.* 2019; **174**:292–308.
2. Kryshchyshyn-Dylevych A, Garazd M, Karkhut A, Polovkovych S, Lesyk R. Synthesis and anticancer activity evaluation of 3-(4-oxo-2-thioxothiazolidin-5-yl)-1H-indole-carboxylic acids derivatives. *Synth Commun.* 2020; **50**(18):2830–8.
3. Mendel D, Laird D, Xin X, Louie S, Christensen J, Li G, Schreck R, Abrams T, Ngai T, Lee T, Murray L, Carver J, Chan E, Moss K, Haznedar J, Sukbuntherng J, Blake R, Sun L, Tang C, Miller T, Shirazian S, McMahon G, Cherrington, J. In vivo antitumor activity of SU11248, a novel tyrosine kinase inhibitor targeting vascular endothelial growth factor and platelet-derived growth factor receptors: determination of a pharmacokinetic/pharmacodynamic relationship. *Clin Cancer Res.* 2003; **9**(1):327–37.
4. Haddad J. The immunopharmacologic potential of Semaxanib and new generation directed therapeutic drugs: Receptor tyrosine kinase regulation with anti-tumorigenesis/angiogenesis properties. *Saudi Pharm J.* 2012; **20**(2):103–23.
5. Laird D, Vajkoczy P, Shawver L, Thurnher A, Liang C, Mohammadi M, Schlessinger J, Ullrich A, Hubbard S, Blake R, Fong A, Strawn L, Sun L, Tang C, Hawtin R, Tang F, Shenoy N, Hirth P, McMahon G, Cherrington J. SU6668 is a potent antiangiogenic and antitumor agent that induces regression of established tumors. *Cancer Res.* 2000; **60**(15):4152–60.
6. Patil R, Patil S, Beaman K, Patil S. Indole Molecules as Inhibitors of Tubulin Polymerization: potential New Anticancer Agents, an Update (2013–2015). *Future Med Chem.* 2016; **8**:1291–316.

7. Granchi C, Roy S, De Simone A, Salvetti I, Tuccinardi T, Martinelli A, Macchia M, Lanza M, Betti L, Giannaccini G, Lucacchini A, Giovannetti E, Sciarillo R, Peters G, Minutolo F. N-Hydroxyindole-Based Inhibitors of Lactate Dehydrogenase against Cancer Cell Proliferation. *Eur J Med Chem.* 2011; **46**:5398–407.
8. Fouad M, Zaki M, Lotfy R, Wala M. Insight on a new indolinone derivative as an orally bioavailable lead compound against renal cell carcinoma. *Bioorg Chem.* 2021; **112**:104985.
9. Kryshchshyn-Dylevych A, Radko L, Finiuk N, Garazd M, Kashchak N, Posyniak A, Niemczuk K, Stoika, Lesyk R. Synthesis of novel indole-thiazolidinone hybrid structures as promising scaffold with anticancer potential. *Bioorg Med Chem.* 2021; **50**:116453.
10. Subtelna I, Kryshchshyn-Dylevych A, Jia R, Lelyukh M, Ringler A, Kubicek S, Zagrijtschuk O, Kralovics R, Lesyk R. 5-Arylidene-2-(4-hydroxyphenyl)aminothiazol-4(5H)-ones with selective inhibitory activity against some leukemia cell lines. *Arch Pharm.* 2021; **354**(4):2000342.
11. Szychowski K, Skóra B, Kryshchshyn-Dylevych A, Kaminskyy D, Rybczyńska-Tkaczyk K, Lesyk R, Gmiński J. Induction of Cyp450 enzymes by 4-thiazolidinone-based derivatives in 3T3-L1 cells in vitro. *Naunyn-Schmiedeb Arch Pharmacol.* 2021; **394**(5):915–27.
12. Monks A, Scudiero D, Skehan P, Shoemaker R, Paull K, Vistica D, Hose C, Langley J, Cronise P, Vaigro-Wolff A, Gray-Goodrich M, Campbell H, Mayo J, Boyd M. Feasibility of a high-flux anticancer drug screen using a diverse panel of cultured human tumor cell lines. *J Natl Cancer Inst.* 1991; **83**:757–66.
13. Boyd M, Paull K. Some practical considerations and applications of the national cancer institute in vitro anticancer drug discovery screen. *Drug Dev Res.* 1995; **34**:91–109.
14. Boyd M. The NCI In Vitro Anticancer Drug Discovery Screen in: Teicher BA. Cancer Drug Discovery and Development, Vol. 2, Humana Press, Totowa, New York, 1997: 23–43.
15. Li Q, Yin X, Wang W, Zhan M, Zhao B, Hou Z, Wang J. The effects of buthionine sulfoximine on the proliferation and apoptosis of biliary tract cancer cells induced by cisplatin and gemcitabine. *Oncol Lett.* 2016; **11**(1):474–80.
16. Mosmann T. Rapid colorimetric assay for cellular growth and survival: application to proliferation and cytotoxicity assay. *J Immunol Methods.* 1983; **65**(1–2):55–63.
17. Radko L, Stypula-Trębas S, Posyniak A, Zyro D, Ochocki J. Silver(I) complexes of the pharmaceutical agents metronidazole and 4-hydroxymethylpyridine: comparison of cytotoxic profile for potential clinical application. *Molecules.* 2019; **24**(10):1949.
18. Borenfreund E, Puerner J. Toxicity determined *in vitro* by morphological alterations and neutral red absorption. *Toxicol Lett.* 1985; **24**(2–3):119–124.
19. Bradford M. A rapid and sensitive method for the quantitation of microgram quantities of protein using the principle of dye binding. *Anal Biochem.* 1976; **72**(1–2):248–54.
20. Korzeniewski C, Calleawert D. An enzyme-release assay for natural cytotoxicity. *J Immunol Method.* 1983; **64**(3): 313–20.
21. Badisa R, Darling-Reed S, Joseph P, Cooperwood J, Latinwo L, Goodman C. Selective cytotoxic activities of two novel synthetic drugs on human breast carcinoma MCF-7 cells. *Anticancer Res.* 2009; **29**(8):2993–6.
22. Peña-Morán OA, Villarreal ML, Álvarez-Berber L, Meneses-Acosta A, Rodríguez-López V. Cytotoxicity, Post-Treatment Recovery, and Selectivity Analysis of Naturally Occurring Podophyllotoxins from *Bursera fagaroides* var. *fagaroides* on Breast Cancer Cell Lines. *Molecules.* 2016;**21**(8):1013.
23. Morris G, Goodsell D, Halliday R, Huey R, Hart W, Belew R, Olson A. Automated docking using a Lamarckian genetic algorithm and an empirical binding free energy function. *J Comput Chem.* 1998; **19**(14):1639–62.
24. Bold G, Schnell C, Furet P, McSheehy P, Brügggen J, Mestan J, Manley P, Drückes P, Burglin M, Dürler U, Loretan J, Reuter R, Wartmann M, Theuer A, Bauer-Probst B, Martiny-Baron G, Allegrini P, Goeppfert A, Wood J, Littlewood-Evans, A. A novel potent oral series of VEGFR2 inhibitors abrogate

- tumor growth by inhibiting angiogenesis. *J Med Chem.* 2016; **59**(1):132–46.
25. Chen H, Deng S, Albadari N, Yun M, Zhang S, Li Y, Ma D, Parke D, Yang L, Seagroves T, White S, Miller D, Li, W. Design, synthesis, and biological evaluation of stable colchicine-binding site tubulin inhibitors 6-Aryl-2-benzoyl-pyridines as potential anticancer agents. *J Med Chem.* 2021; **64**(16):12049–74.
 26. Debs G, Cha M, Liu X, Huehn A, Sindelar C. Dynamic and asymmetric fluctuations in the microtubule wall captured by high-resolution cryoelectron microscopy. *Proc Natl Acad Sci.* 2020; **117**(29):16976–84.
 27. Waight A, Bargsten K, Doronina S, Steinmetz M, Sussman D, Protá A. Structural basis of microtubule destabilization by potent auristatin anti-mitotics. *PLoS One.* 2016; **11**(8):e0160890.
 28. Tang J, Wang Y, Zhou H, Ye Y, Talukdar M, Fu Z, Liu Z, Li J, Neculai D, Gao J, Huang H. Sunitinib inhibits RNase L by destabilizing its active dimer conformation. *Biochem J.* 2020; **477**(17):3387–99.
 29. Gajiwala K, Wu J, Christensen J, Deshmukh G, Diehl W, DiNitto J, English J, Greig M, He Y-A, Jacques S, Lunney E, McTigue M, Molina D, Quenzer T, Wells P, Yu X, Zhang Y, Zou A, Emmett M, Marshall A, Zhang H-M, Demetri G. KIT kinase mutants show unique mechanisms of drug resistance to imatinib and sunitinib in gastrointestinal stromal tumor patients. *Proc Natl Acad Sci USA.* 2009; **106**(5):1542–7.
 30. Zhang J, Adrián F, Jahnke W, Cowan-Jacob S, Li A, Iacob R, Sim T, Powers J, Dierks C, Sun F, Guo G-R, Ding Q, Okram B, Choi Y, Wojciechowski A, Deng X, Liu G, Fendrich G, Strauss A, Vajpai N, Grzesiek S, Tuntland T, Liu Y, Bursulaya B, Azam M, Manley P, Engen J, Daley G, Warmuth M, Gray N. Targeting Bcr–Abl by combining allosteric with ATP-binding-site inhibitors. *Nature.* 2010; **463**(7280): 501–6.
 31. Morris G, Huey R, Lindstrom W, Sanner M, Belew R, Goodsell D, Olson A. AutoDock4 and AutoDockTools4: Automated docking with selective receptor flexibility. *J Comput Chem.* 2009; **30**(16):2785–91.
 32. Pettersen E, Goddard T, Huang C, Couch G, Greenblatt D, Meng E, Ferrin T. UCSF chimera — a visualization system for exploratory research and analysis. *J Comput Chem.* 2004; **25**(13):1605–12.
 33. Wolber G, Langer T. LigandScout: 3-D pharmacophores derived from protein-bound ligands and their use as virtual screening filters. *J Chem Inf Model.* 2005; **45**(1):160–9.
 34. Kaminskyy D, Kryshchyshyn A, Lesyk R. Recent developments with rhodanine as a scaffold for drug discovery. *Expert Opin Drug Discov.* 2017; **12**(12):1233–52.
 35. Kryshchyshyn A, Kaminskyy D, Roman O, Kralovics R, Karpenko O, Lesyk R. Synthesis and anti-leukemic activity of pyrrolidinedione-thiazolidinone hybrids. *Ukr Biochem J.* 2020; **92**(2):108–19.
 36. Subtel'na I, Atamanyuk D, Szymanska E, Kieckonowicz K, Zimenkovsky B, Vasylenko O, Gzella A, Lesyk R. Synthesis of 5-arylidene-2-amino-4-azolones and evaluation of their anticancer activity. *Bioorg Med Chem.* 2010; **14**:5090–102.
 37. Mobinikhaledi A, Amiri A. Natural eutectic salts catalyzed one-pot synthesis of 5-arylidene-2-imino-4-thiazolidinones. *Res Chem Intermed.* 2013; **39**:1491–8.
 38. Havrylyuk D, Zimenkovsky B, Vasylenko O, Gzella A, Lesyk R. Synthesis of new 4-thiazolidinone-, pyrazoline-, and isatin-based conjugates with promising antitumor activity. *J Med Chem.* 2012; **55**:8630–41.
 39. Kaminskyy D, Den Hartog G, Wojtyra M, Lelyukh M, Gzella A, Bast A, Lesyk R. Antifibrotic and anticancer action of 5-ene amino/iminothiazolidinones. *Eur J Med Chem.* 2016; **112**:180–95.
 40. Nowaczyk A, Kowiel M, Gzella A, Fijałkowski L, Horishny V, Lesyk R. Conformational space and vibrational spectra of 2-[(2,4-dimethoxyphenyl)amino]-1,3-thiazolidin-4-one. *J Mol Model.* 2014; **20**(8):2366.
 41. Kaminskyy D, Subtel'na I, Zimenkovsky B, Karpenko O, Gzella A, Lesyk R. Synthesis and evaluation of anticancer activity of 5-ylidene-4-aminothiazol-2(5H)-one derivatives. *Med Chem.* 2015; **11**(6):517–30.
 42. Pyrih A, Jaskolski M, Gzella A, Lesyk R. Synthesis, structure and evaluation of anticancer activity of 4-amino-1,3-thiazolinone/pyrazoline hybrids. *J Mol Struct.* 2021; **1224**:129059.
 43. Skóra B, Lewińska A, Kryshchyshyn-Dylevych A, Kaminskyy D, Lesyk R, Szychowski K. Evaluation

of anticancer and antibacterial activity of four 4-thiazolidinone-based derivatives. *Molecules*. 2022; **27**(3):894.

44. Rehulka J, Subtelna I, Kryshchyshyn-Dylevych A, Cherniienko A, Ivanova A, Matveieva M, Polishchuk P, Gurska S, Hajduch M, Zagrijtschuk O, Dzubak P, Lesyk R. Anticancer 5-arylidene-2-(4-hydroxyphenyl) aminothiazol-4(5H)-ones as tubulin inhibitors. *Arch Pharm*. 2022;**355**(12) e2200419.

Противухлинна цитотоксичність індол-тіазолідинонових гібридів та *in silico* дослідження механізму їх дії

А. П. Крищишин-Дилевич, І. Ю. Субтельна, Н. С. Фінюк, Л. Радко, А. Павелчик, Р. С. Стойка, Р. Б. Лесик

Мета. Спрямований дизайн та синтез нових гібридних молекул, що містять [6+5]-гетероцикли та тіазолідиноновий фрагмент, а також вивчення їх як потенційних протиракових агентів. **Методи.** Органічний синтез, біологічні дослідження *in vitro*, аналіз взаємозв'язку структура-активність, молекулярний докінг, фармакофорне моделювання. **Результати.** Здійснено дизайн та синтез серії нових синтетичних гібридів тіазолідинон-індол-карбоксилатів та вивчено їх токсичність до ліній гепатокарциноми (HepG2), гліобластоми (U251), аде-

нокарциноми молочної залози (MCF-7) та промієлоцитарної лейкемії (HL-60) людини. Клітинні лінії гепатокарциноми, гліобластоми та аденокарциноми молочної залози були слабо чутливі до досліджуваних сполук, 5-флюоро-3-[2-(4-гідроксианіліно)-4-оксо-тіазол-5-іліден]метил]-1*H*-індол-2-карбоксилат інгібував життєздатність лінії промієлоцитарної лейкемії HL-60 у мікромолекулярній концентрації $IC_{50} = 8.36$ мкМ. Дослідження цитотоксичної дії цієї сполуки на панелі ліній клітин раку показало, що найбільш чутливими були лінії клітин лейкемії, меланоми та раку яйників. **Висновки.** *In vitro* дослідження біологічних ефектів синтезованих речовин дозволило ідентифікувати сполуку-хіт **2c** з протилейкемічною дією та низькою токсичністю до псевдонормальних фібробластів мишей (Balb/c3T3). В цілому, 4-тіазолідинон-індолкарбоксилат **2c** інгібує життєздатність 21-єї лінії ракових клітин більше, ніж на 50 %. Вивчення *in silico* ймовірних механізмів зв'язування сполуки-хіта **2c** показало її високу афінність до колхіцинового сайту тубуліну.

Ключові слова: 1*H*-індол, тіазолідин, синтез, протиракова активність, SAR аналіз, *in silico* дослідження.

Received 03.12.2022